18th International Conference
ENGINEERING MECHANICS 2012
Svratka, Czech Republic, May 14 – 17, 2012

pp. 1017–1031
Paper #54

VALIDATION OF THE POINT-MASS MODELLING APPROACH FOR FIBRES IN THE INVERTED PENDULUM MODEL

P. Polach[*], M. Hajžman[**], O. Tuček[***]

Abstract: *Fibres, cables and wires can play an important role in design of many machines. One of interesting applications is replacing the chosen rigid elements of a manipulator or a mechanism with fibres. The main advantage of this design is achievement of a lower moving inertia, which can lead to a higher mechanism speed and lower production costs. A chosen inverted pendulum attached to a frame by two fibres serves as a typical testing system for the investigation of the fibres properties influence on the system dynamic response. Motion of the pendulum of this nonlinear system is investigated using the* ***alaska*** *simulation tool. The sophisticated point-mass fibre model is validated on the basis of the results obtained using a massless fibre model. In addition, the equation of motion based on the massless approach is studied in terms of solution existence and its uniqueness.*

Keywords: ***Inverted pendulum, fibres, multibody modelling, vibration.***

1. Introduction

One of interesting applications of cables or fibres is replacement of the chosen rigid elements of manipulators or mechanisms by those flexible elements (Chan, 2005). The main advantage of this design is the achievement of a lower moving inertia, which can lead to a higher machine speed and lower production costs. Drawbacks can be associated with the fact that cables should be only in tension (Smrž & Valášek, 2009; Valášek & Karásek, 2009) in the course of a motion. The possible cable modelling approaches should be tested and their suitability verified in order to create efficient mathematical models of cable-based manipulators mainly intended for the control algorithm design. The motion of the inverted pendulum driven by two fibres attached to a frame (see Fig. 1), which is a simplified representation of a typical cable manipulator, is investigated using the **alaska** simulation tool (and using an in-house software created in the MATLAB system). The influence of some parameters of this system has already been investigated. The influence of the actuated fibres motion on the pendulum motion in the case of their simultaneous harmonic excitation was investigated in Polach & Hajžman (2011c), in the case of non-symmetric harmonic excitation it was investigated in Polach & Hajžman (2012a). The effect of the fibres' mass on the pendulum motion was investigated in Polach et al. (2012), the effect of the fibres preload was investigated in Polach & Hajžman (2012b).

The sophisticated point-mass fibre model is validated on the basis of the results obtained using a massless fibre model. The correctness of the point-mass fibre model is partly evident from Polach et al. (2012), where results of simulations when considering relatively "light" fibre made of thin carbon fibres correspond well, up to the certain excitation frequency, with the results of simulations with massless fibre model (see also Chapter 5). In addition, in this paper the equation of motion based on the massless approach is studied in terms of solution existence and its uniqueness.

[*] Dr. Ing. Pavel Polach: Section of Materials and Mechanical Engineering Research, Výzkumný a zkušební ústav Plzeň s.r.o., Tylova 1581/46; 301 00, Plzeň; CZ, e-mail: polach@vzuplzen.cz

[**] Ing. Michal Hajžman, Ph.D.: Department of Computer-Aided Modelling, Výzkumný a zkušební ústav Plzeň s.r.o., Tylova 1581/46; 301 00, Plzeň; CZ, e-mail: hajzman@vzuplzen.cz

[***] Mgr. Ondřej Tuček: Department of Computer-Aided Modelling, Výzkumný a zkušební ústav Plzeň s.r.o., Tylova 1581/46; 301 00, Plzeň; CZ, e-mail: tucek@vzuplzen.cz

2. Possibilities of the cable modelling

The cable (fibre, wire etc.) modelling (Hajžman & Polach, 2011) should be based on considering the cable flexibility and the suitable approaches can be based on the flexible multibody dynamics (see Shabana, 1997). The simplest way how to incorporate cables in equations of motion of a mechanism is the force representation of a cable (e.g. Diao & Ma, 2009). It is assumed that the mass of cables is small to such an extent comparing to the other moving parts that the inertia of cables is negligible with respect to the other parts. The cable is represented by the force dependent on the cable deformation and its stiffness and damping properties. This way of the cable modelling is probably the most frequently used model in the cable-driven robot dynamics and control.

A more precise approach is based on the representation of the cable by a point-mass model (e.g. Kamman & Huston, 2001). The cable can be considered either flexible or rigid. It has the advantage of a lumped point-mass model. The point masses can be connected by forces or constraints.

In order to represent bending behaviour of cables their discretization using the finite segment method (Shabana, 1997) or so called rigid finite elements (Wittbrodt et al., 2006) is possible. Standard multibody codes (SIMPACK, MSC.ADAMS, **alaska** etc.) can be used for this purpose. Other more complex approaches can utilize nonlinear three-dimensional finite elements (Freire & Negrão, 2006) or can employ the absolute nodal coordinate formulation (ANCF) elements (Shabana, 1997).

Investigation of the possible approaches to the modeling of the system of inverted pendulum driven by fibres was investigated in Polach & Hajžman (2011a) and Polach & Hajžman (2011b). Implementation of the model based on the finite rigid elements into the **alaska** simulation tool proved to be unsuitable (Polach & Hajžman, 2011a). The ANCF elements cannot be implemented in the **alaska** simulation tool, verification on this approach was carried out utilizing the MATLAB system (Polach & Hajžman, 2011b).

3. Inverted pendulum

Already mentioned inverted pendulum, which is attached and driven by two fibres and affected by a gravitation force, was chosen as an example of the investigation of fibres' behaviour – see Fig. 1. When the pendulum is displaced from the equilibrium position (i.e. "upper" position) it is returned back to the equilibrium position by the tightened fibre.

The massless model is shown in Fig. 1 (the used model of the fibre based on the point-mass model with lumped point masses corresponding to the mass of the fibre is geometrically identical) – e.g. Polach & Hajžman (2011c). The models of the system of the inverted pendulum are considered to be two-dimensional.

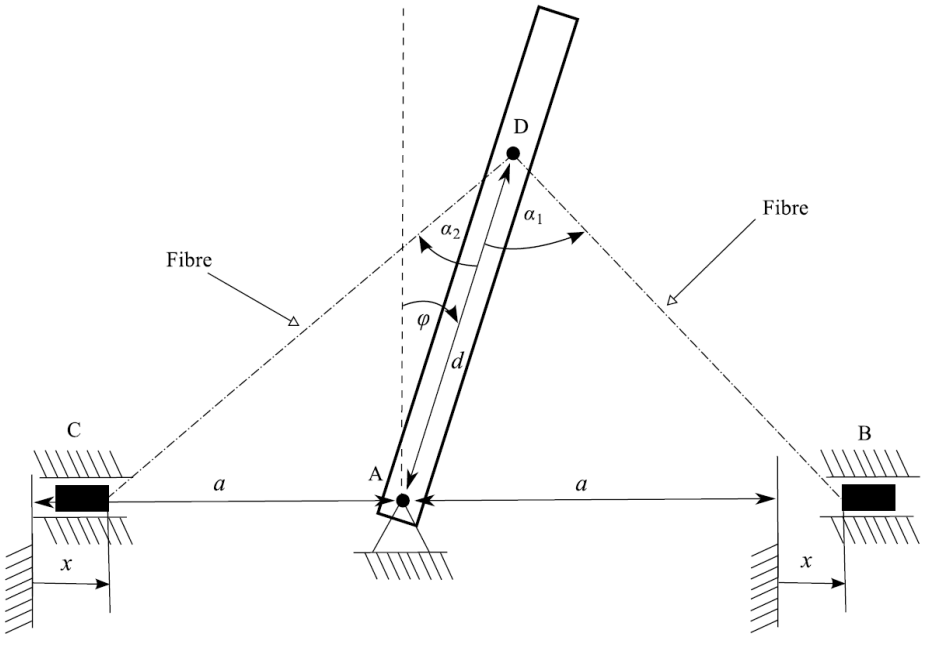

Fig. 1: Inverted pendulum actuated by the fibres.

The system kinematics can be described by angle φ (one degree of freedom) and prescribed kinematic excitation $x(t)$. The equation of motion is of the form

$$\ddot{\varphi} = \frac{1}{I_{\mathrm{A}}} \cdot \left(F_1(\varphi) \cdot d \cdot \sin \alpha_1(\varphi) - F_2 \cdot d \cdot \sin \alpha_2(\varphi) + m \cdot g \cdot \frac{l}{2} \cdot \sin \varphi \right), \tag{1}$$

where I_{A} is the moment of inertia of the pendulum with respect to the axis in point A (see Fig. 1), $\alpha_1(\varphi)$ and $\alpha_2(\varphi)$ are angles between the pendulum and the fibres, m is the mass of the pendulum, g is the gravity acceleration and l is the length of the pendulum. The forces acting on the pendulum from the fibre are

$$\begin{aligned} F_1(\varphi) &= \left[k_1 \cdot \left(l_1(\varphi) - l_0 \right) + b_1 \cdot \frac{\mathrm{d}l_1(\varphi)}{\mathrm{d}t} \right] \cdot H\left(l_1(\varphi) - l_0 \right), \\ F_2(\varphi) &= \left[k_2 \cdot \left(l_2(\varphi) - l_0 \right) + b_2 \cdot \frac{\mathrm{d}l_2(\varphi)}{\mathrm{d}t} \right] \cdot H\left(l_2(\varphi) - l_0 \right), \end{aligned} \tag{2}$$

where k_i (i = 1, 2) is the fibre stiffness, b_i (i = 1, 2) is the fibre damping coefficient and $H(\cdot)$ is the Heaviside function. It is supposed, that forces act in the fibres only when the fibres are in tension.

Original length l_0 of the fibres is supposed to be constant and actual lengths $l_1(\varphi)$ and $l_2(\varphi)$ of the fibres should be calculated in each time

$$\begin{aligned} l_1(\varphi) &= \sqrt{\left(d \cdot \cos \varphi \right)^2 + \left(a + x(t) - d \cdot \sin \varphi \right)^2}, \\ l_2(\varphi) &= \sqrt{\left(d \cdot \cos \varphi \right)^2 + \left(a - x(t) + d \cdot \sin \varphi \right)^2}. \end{aligned} \tag{3}$$

Each fibre is discretized using 10 point masses in the fibre model based on the point masses (e.g. Polach & Hajžman, 2011c). Each point mass is unconstrained (i.e. number of degree of freedom is 3) in two-dimensional model of the system of the inverted pendulum. The adjacent point masses are connected using spring-damper elements. Only axial (spring and damping) forces are considered in these spring-damper elements. The stiffness and the damping between the masses are determined in order to keep the global properties of the massless fibre model.

The kinematic excitation is given by function

$$x(t) = x_0 \cdot \sin\left(2 \cdot \pi \cdot f \cdot t \right), \tag{4}$$

where x_0 is the chosen amplitude of motion, f is the excitation frequency and t is time. The influence of the excitation frequency on the pendulum motion is investigated. Excitation in points designated B and C (see Fig. 1) is considered to be symmetrical (without any mutual phase shift) and of the same amplitude x_0.

4. Existence and uniqueness of the solution of the pendulum motion equation

Before the validation of the point-mass fibre model the existence and uniqueness of the solution should be studied. For sake of such an analysis the pendulum equation of motion based on the fibre modelling by massless approach (1) can be rewritten to form

$$\begin{aligned} &\ddot{\varphi}(t) = f\left(t, \varphi, \dot{\varphi} \right), \\ &\varphi(0) = 0, \\ &\varphi(T) = 0, \\ &t \in \left[0, T \right], \end{aligned} \tag{5}$$

where

$$f\left(t, \varphi, \dot{\varphi} \right) = B_0 \cdot F_1(\varphi) \cdot \sin \alpha_1(\varphi) - B_0 \cdot F_2(\varphi) \cdot \sin \alpha_2(\varphi) + B_1 \cdot \sin \varphi, \tag{6}$$

$$\sin\alpha_1(\varphi)=\frac{\cos\varphi}{l_1(\varphi)}\cdot\big(a+x(t)\big),$$
$$\sin\alpha_2(\varphi)=\frac{\cos\varphi}{l_2(\varphi)}\cdot\big(a-x(t)\big), \tag{7}$$
$$B_0=\frac{d}{I_A},\quad B_1=\frac{m\cdot g\cdot l}{2\cdot I_A},$$

$F_1(\varphi)$ and $F_2(\varphi)$ are given by expressions (2), $l_1(\varphi)$ and $l_2(\varphi)$ are given by expressions (3) and T is the time of the end of numerical simulation.

Function $x(t)$ is considered to be smooth function of property

$$\left|\dot{x}(t)\right|\le\tilde{K}\,. \tag{8}$$

From previous estimate it is easy to derive the following condition

$$\left|x(t)\right|\le K\,,$$

where from the physical point of view constant K fulfills

$$d-a<K<d+a\,.$$

Constants a, d, l_0, $\tilde{K}$, K, k_i (i = 1, 2), b_i (i = 1, 2) in equations (1), (2), (3), (8) are positive real numbers.

It is reasonable to suppose that velocity of pendulum is bounded, i.e. there is a positive constant R such that

$$\left|\dot{\varphi}(t)\right|\le R\,. \tag{9}$$

Based on expression (2) it can be seen that $F_i(\varphi)$ (i = 1, 2) is discontinuous due to appearing the Heaviside function. Hence function $f(t,\varphi,\dot{\varphi})$ on the right hand side of (5) is also discontinuous and nonlinear. Thus it is obvious that there is no solution for $\varphi\in C^2$, where C^k, k = 2, is space of all functions such that the k-th derivative exists and is continuous.

4.1. Preliminaries

Throughout this section a notation $|\cdot|$ for absolute value in $\mathbb{R}$ and space

$$C_0^1\big([0,T]\big)=\big\{u\in C^1\big([0,T],\mathbb{R}\big):u(t)=0,\ t\in\{0,T\}\big\}$$

will be used.

Let $T>0$ be given and let

$$f(t,u,v):[0,T]\times\mathbb{R}\times\mathbb{R}\to\mathbb{R}$$

be a mapping satisfying the Carathéodory conditions (e.g. Drábek & Milota, 2007; Rachůnková et al., 2009), which are

1. $f(t,u,v)$ is continuous in (u,v) for almost all $t\in[0,T]$,
2. $f(t,u,v)$ is measurable in t for fixed (u,v),
3. for each compact set $\kappa\subset\mathbb{R}^2$, there is a function $h(t)\in L_1\big([0,T]\big)$ such that

$$\left|f(t,u,v)\right|\le h(t)\ \text{for a.e. } t\in[0,T]\ \text{and all } (u,v)\in\kappa, \tag{10}$$

where L_1 is space of measurable functions such that $\int_0^T\left|h(t)\right|\cdot dt<\infty$.

Following theorems with proofs can be found in Rachůnková et al. (2009) and Schmitt & Thompson (2004).

Theorem 1 *Let* $f(t,u,v)$ *satisfy the Carathéodory conditions and assume that there is a function* $h(t)\in L_1([0,T])$ *such that*

$$\left|f(t,u,v)\right|\le h(t) \text{ for a.e. } t\in[0,T] \text{ and } \forall u,v\in\mathbb{R}. \tag{11}$$

Then problem (5) has a solution.

Theorem 2 *Let* $f(t,u,v)$ *satisfy the Carathéodory conditions and*

$$\left|f(t,u,v)-f(t,\overline{u},\overline{v})\right|\le A_0\cdot\left|u-\overline{u}\right|+A_1\cdot\left|v-\overline{v}\right|,\ \forall u,v,\overline{u},\overline{v}\in\mathbb{R},t\in[0,T], \tag{12}$$

where A_0, A_1 *are positive constants such that*

$$\frac{A_0\cdot T^2}{\pi^2}+\frac{A_1\cdot T}{\pi}<1. \tag{13}$$

Then problem (5) has a unique solution $\varphi\in C_0^1([0,T])$*, with* $\dot{\varphi}$ *absolutely continuous and equation (5) being satisfied almost everywhere.*

4.2. Main qualitative result

The solvability of problem (5) is investigated in this subchapter. It is known that there exist points in $[0,T]$ where function $f(t,u,v)$ is discontinuous and the Lebesgue measure of the set of these points is equal zero. Thus for almost all $t\in[0,T]$ is $f(t,u,v)$ continuous, it means the first condition of the Carathéodory conditions is satisfied. The second condition is obviously satisfied, too.

Now if the same *R* as in (9) is used $\kappa=[-R,R]\times[-R,R]$ can be chosen. Then the inequality (10) will be fulfilled with $h(t)$ in the form

$$\begin{aligned}\left|f(t,u,v)\right|&\le B_0\cdot\left|F_1(u,v)\cdot\frac{\cos u}{l_1(u)}\right|\cdot\left|a+x(t)\right|+B_0\cdot\left|F_2(u,v)\cdot\frac{\cos u}{l_2(u)}\right|\cdot\left|a-x(t)\right|+B_1\\&\le\left(C_0+C_1+(C_2+C_3)\cdot\left(d\cdot R\cdot(a+K)+\tilde{K}\cdot(a+K)+d\cdot\tilde{K}\right)\right)\cdot(a+K)=h(t),\end{aligned} \tag{14}$$

where

$$\begin{aligned}&C_0=B_0\cdot k_1\cdot\left(1+\frac{l_0}{\left|K+(a-d)\right|}\right),\quad C_1=B_0\cdot k_2\cdot\left(1+\frac{l_0}{\left|K-(a-d)\right|}\right),\\&C_2=\frac{B_0\cdot b_1}{\left(K+(a-d)\right)^2},\quad C_3=\frac{B_0\cdot b_2}{\left(K-(a-d)\right)^2}\quad,\end{aligned} \tag{15}$$

so $h(t)$ is element of L_1. Therefore $f(t,u,v)$ satisfies the Carathéodory conditions and assumptions of Theorem 1 too.

Condition (12) of Theorem 2 remains to be checked. It holds

$$\begin{aligned}&\left|f(t,u,v)-f(t,\overline{u},\overline{v})\right|\le B_0\cdot\left|F_1(u,v)\cdot\frac{\cos u}{l_1(u)}\cdot\left(a+x(t)\right)-F_1(\overline{u},\overline{v})\cdot\frac{\cos\overline{u}}{l_1(\overline{u})}\cdot\left(a+x(t)\right)-\right.\\&\left.\left(F_2(u,v)\cdot\frac{\cos u}{l_2(u)}\cdot\left(a-x(t)\right)-F_2(\overline{u},\overline{v})\cdot\frac{\cos\overline{u}}{l_2(\overline{u})}\cdot\left(a-x(t)\right)\right)\right|+B_1\cdot\left|\sin u-\sin\overline{u}\right|\le\\&B_0\cdot\left|\left|(-d)\cdot(v-\overline{v})\right|\cdot\frac{b_1\cdot(a+K)^2}{\left(K+(a-d)\right)^2}+\left|d\cdot(v-\overline{v})\right|\cdot\frac{b_2\cdot(a+K)^2}{\left(K-(a+d)\right)^2}\right|+B_1\cdot\left|u-\overline{u}\right|=\\&B_1\cdot\left|u-\overline{u}\right|+B_0\cdot\left(\frac{d\cdot b_1\cdot(a+K)^2}{\left(K+(a-d)\right)^2}+\frac{d\cdot b_2\cdot(a+K)^2}{\left(K-(a+d)\right)^2}\right)\cdot\left|v-\overline{v}\right|\quad.\end{aligned} \tag{16}$$

In estimations (14) and (16) inequalities

$$\left|\sin(\cdot)\right| \le 1, \quad \left|\cos(\cdot)\right| \le 1, \quad \left|\sin u - \sin \bar{u}\right| \le \left|u - \bar{u}\right|, \quad \left|H(\cdot)\right| \le 1,$$
$$\frac{1}{\sqrt{d^2 - 2 \cdot d \cdot \left(a \pm x(t)\right) \cdot \sin u + \left(a \pm x\right)^2}} \le \frac{1}{\left|K \pm (a-d)\right|}, \tag{17}$$

and (9) were used.

It can be seen comparing (13) and (16) that

$$A_0 = B_1$$

and

$$A_1 = d \cdot B_0 \cdot (a+K)^2 \cdot \left(\frac{b_1}{\left(K + (a-d)\right)^2} + \frac{b_2}{\left(K - (a+d)\right)^2} \right). \tag{18}$$

Finally if function $x(t)$ can be chosen such that $\left|x(t)\right| \le K = d$ then one gets

$$A_1 = \frac{d \cdot B_0 \cdot (a+d)^2}{a^2} \cdot (b_1 + b_2). \tag{19}$$

If inequality (13) holds for A_0, A_1 and T it was proven that unique solution

$$\varphi \in C_0^1\left([0,T]\right)$$

of (5) exists.

Now T can be chosen arbitrarily so it might happen that condition (13) would not be satisfied and problem (5) would not have a solution. Thus it is difficult to find or proof other theorem which has less restrictive condition then (13). So if T will be chosen in order to fulfil (13) then a unique solution exists, which is absolutely continuous.

5. Numerical simulations

5.1. Parameters of pendulum models

The most important model parameters (see Fig. 1) are: l = 1 m, a = 1.2 m, d = 0.75 m, I_A = 3.288 kg·m^2, m = 9.864 kg, stiffness k_i = 8.264·10^4 N/m (i = 1, 2), damping coefficient $b_i = 5 \cdot 10^{-4} \cdot k_i$ N·s/m (i = 1, 2). In the case of the point-mass fibre model very low mass of fibre was considered (in contradiction to Polach & Hajžman, 2011a; Polach & Hajžman, 2012b; Polach & Hajžman, 2011c; Polach et al., 2012; Polach & Hajžman, 2012a): mass of one fibre is 0.1 grams. To compare: mass of the so far lightest considered (carbon) real fibre was 3.846 grams – Polach et al. (2012). The natural frequency of the linearized system of the inverted pendulum in equilibrium position at consideration the massless fibre model is 5.04 Hz.

5.2. Verification of the point-mass fibre model

The kinematic excitation amplitude (see Eq. (4)) x_0 = 0.02 m was chosen (as in Polach & Hajžman, 2011a; Polach & Hajžman, 2011c; Polach et al., 2012; Polach & Hajžman, 2012a and Polach & Hajžman, 2012b). Excitation frequency f was considered in the range from 0.1 Hz to 200 Hz.

Time histories and extreme values of pendulum angle φ (maximum value of pendulum angle at quasi-static loading is φ = 1.52°; minimum value of pendulum angle at quasi-static loading is logically φ = –1.52°) are the validated quantities. Selected results of the numerical simulations are presented in Figs 2 to 22. Simulation time is 10 seconds. It was tested that after this period the character of the system response to the kinematic excitation does not change (e.g. Polach & Hajžman, 2011c).

Generally, the pendulum motion is influenced by the excitation frequency of the moving fibres – Polach & Hajžman (2011a); Polach & Hajžman (2011c); Polach et al. (2012); Polach & Hajžman (2012a); Polach & Hajžman (2012b) and Figs 2 to 22.

Extreme values of pendulum angle φ at consideration the massless fibre model and the point-mass fibre model are given in Figs 2 and 3. Absolute differences of pendulum angle φ of point-mass fibre model, i.e. $\left(\varphi_{\text{max massless}} - \varphi_{\text{max point-mass}}\right)$ and $\left(\varphi_{\text{min massless}} - \varphi_{\text{min point-mass}}\right)$, are given in Figs 4 and 5. Relative differences of pendulum angle φ of point-mass fibre model, i.e. $\left(\varphi_{\text{max massless}} - \varphi_{\text{max point-mass}}\right) / \varphi_{\text{max massless}}$ and $\left(\varphi_{\text{min massless}} - \varphi_{\text{min point-mass}}\right) / \varphi_{\text{min massless}}$, are given in Figs 6 and 7 and in Tab. 1. For the purpose of comparing, Figs 2 to 7 show even dependences of plotted quantities of inverted pendulum attached using carbon fibres (Polach et al., 2012). Remarkable time histories of pendulum angle φ at various excitation frequencies are given in Figs 8 to 22.

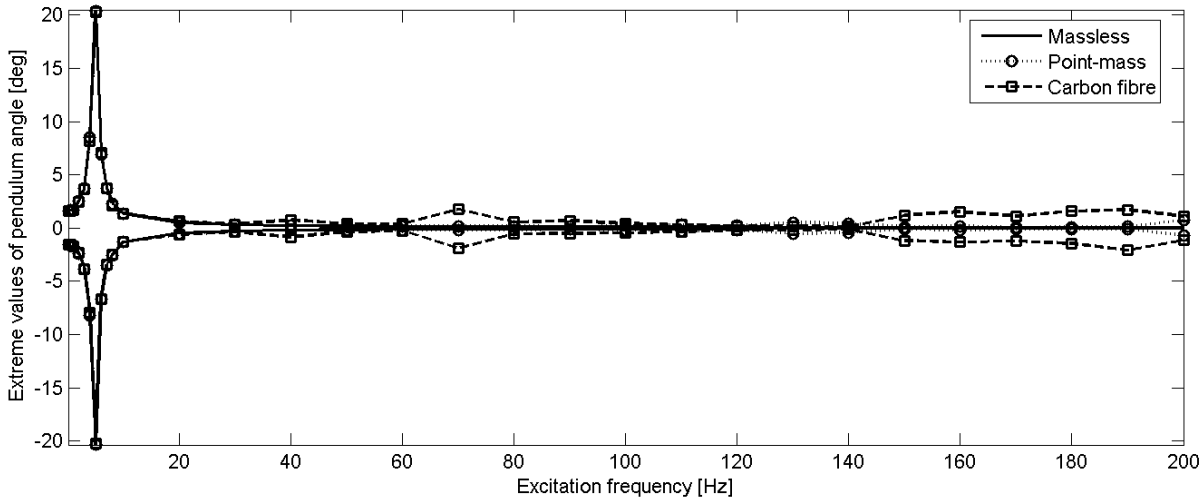

Fig. 2: Extreme values of time histories of pendulum angle φ in dependence on the excitation frequency (in the whole investigated frequency range).

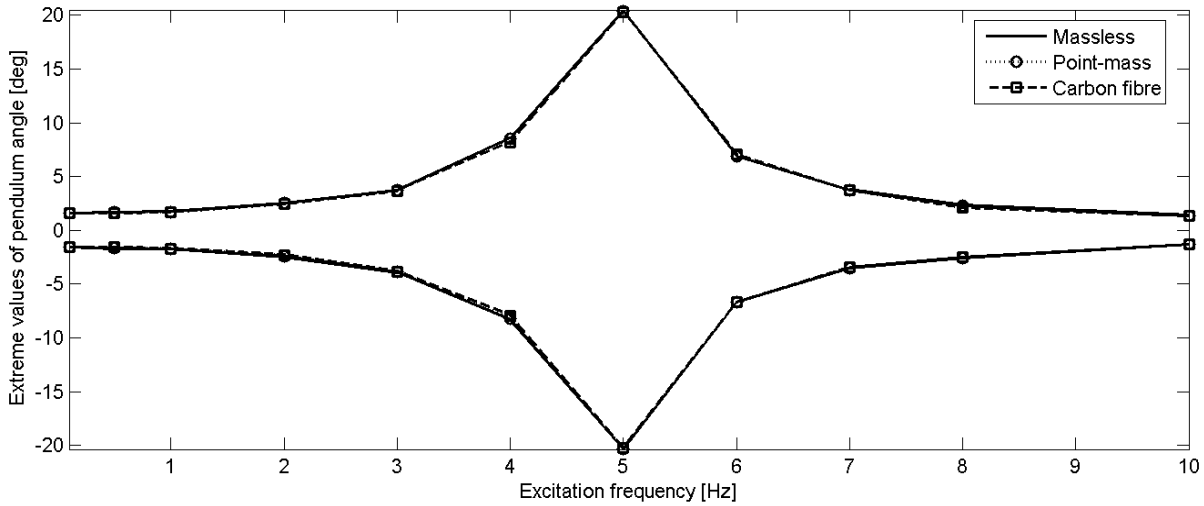

Fig. 3: Extreme values of time histories of pendulum angle φ in dependence on the excitation frequency (up to 10 Hz only).

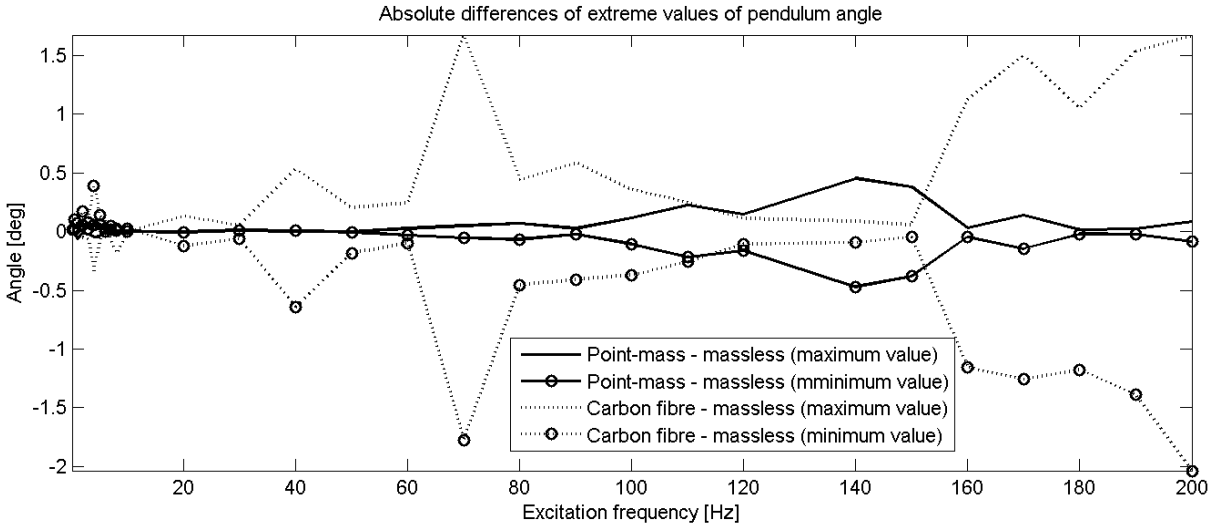

Fig. 4: Absolute differences of extreme values of time histories of pendulum angle φ in dependence on the excitation frequency (in the whole investigated frequency range).

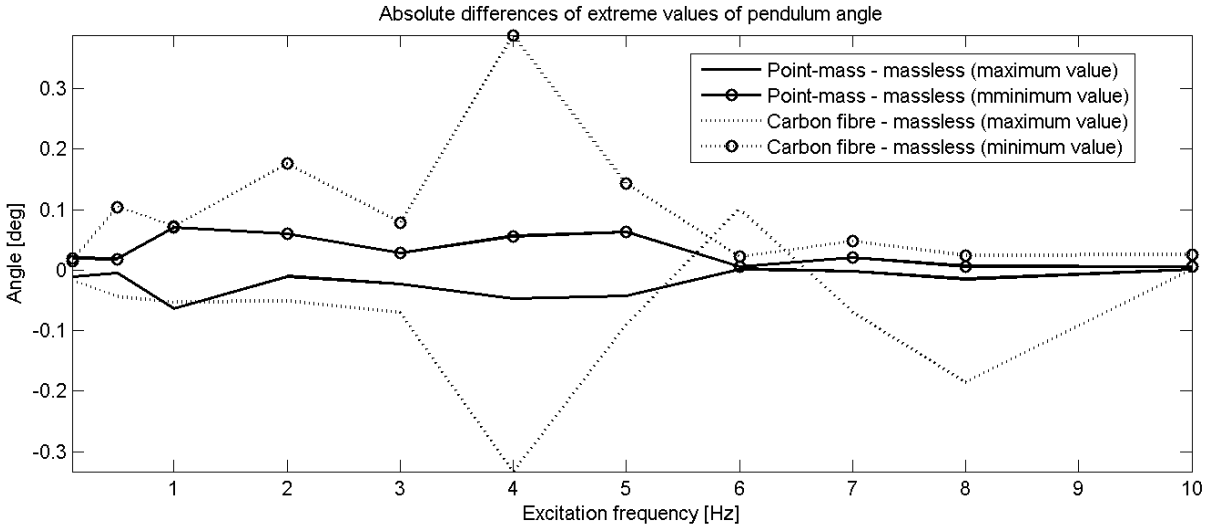

Fig. 5: Absolute differences of extreme values of time histories of pendulum angle φ in dependence on the excitation frequency (up to 10 Hz only).

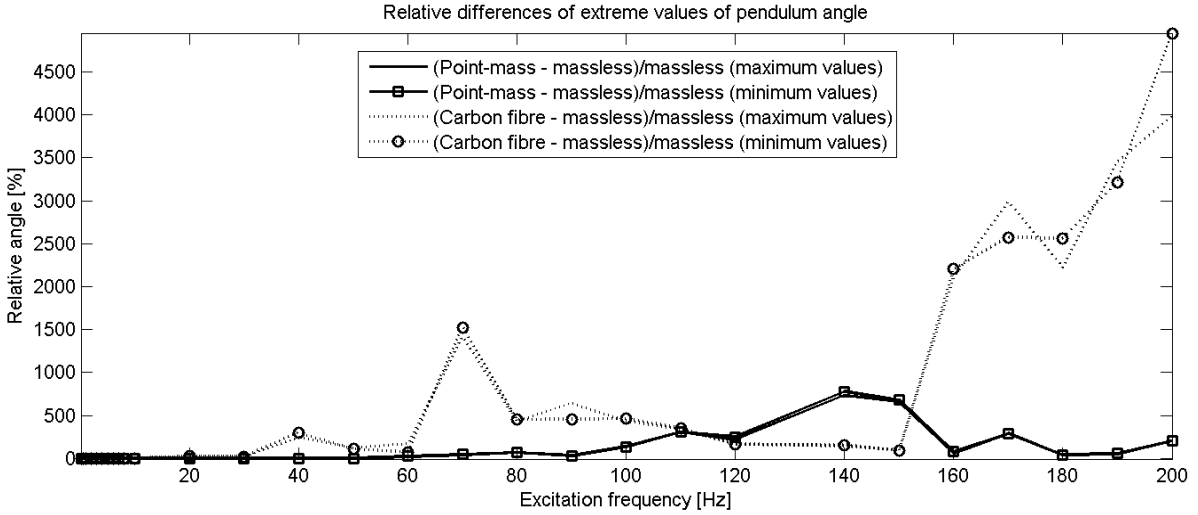

Fig. 6: Relative differences of extreme values of time histories of pendulum angle φ in dependence on the excitation frequency (in the whole investigated frequency range).

Tab. 1: Simulations results.

Excitation frequency f [Hz]	**Relative differences of minimum values of pendulum angle φ [%]**	**Relative differences of maximum values of pendulum angle φ [%]**
0.1	-1.2	-0.7
0.5	-1.1	-0.3
1	-4.0	-3.6
2	-2.4	-0.4
3	-0.7	-0.6
4	-0.7	-0.6
5	-0.3	-0.2
6	-0.1	0
7	-0.6	-0.1
8	-0.3	-0.7
10	-0.4	0.1
20	1.8	0
30	-3.2	3.5
40	-3.3	1.2
50	1.9	-0.1
60	23.4	19.2
70	46.2	42.8
80	65.8	66.1
90	26.5	29.3
100	131.8	142.0
110	303.6	305.1
120	249.7	218.0
140	776.3	734.0
150	678.4	662.9
160	80.4	56.0
170	290.8	277.9
180	39.0	34.3
190	58.4	53.4
200	206.8	206.7

From the courses of the quantities in Figs 2, 4 and 6 and from Tab. 1 it is evident that a good compliance of the results obtained at simulating with inverted pendulum models with the point-mass fibre model and with the massless fibre model is up to the excitation frequencies of approx. 50 Hz (see Figs 2 to 17). At higher excitation frequencies partly vibration of individual point masses and partly probably also influence of numerical errors at solving equations of motion apparently show up in the results of simulations (see Figs 18 to 22). This fact is evident especially from time histories of

pendulum angle φ at excitation frequencies 60 Hz and 70 Hz in Figs 18 and 19, in which time histories of pendulum angle φ of point-mass models with "slightly higher" mass of the "verified" fibre (by 10 %) and when considering carbon fibres are given in addition. Due to the change of the characters of time histories of pendulum angle φ at simulating with inverted pendulum models with the point-mass fibre model and with the massless fibre model (from the excitation frequencies 60 Hz) it is necessary to take the comparison of the extreme values of pendulum angle φ given in Figs 2, 4 and 6 and Tab. 1 cautiously (especially the relative differences of extreme values).

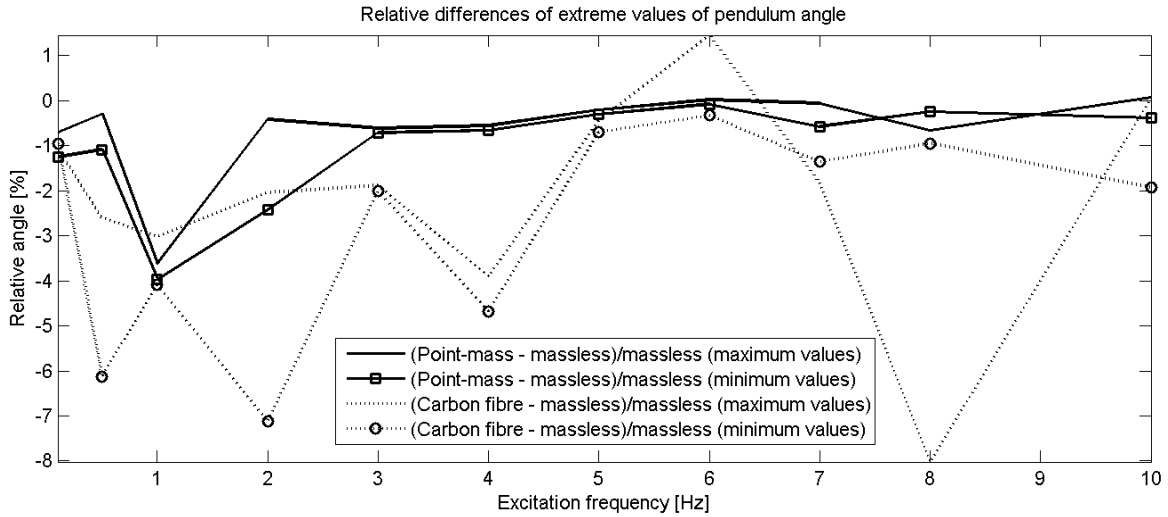

Fig. 7: Relative differences of extreme values of time histories of pendulum angle φ in dependence on the excitation frequency (up to 10 Hz only).

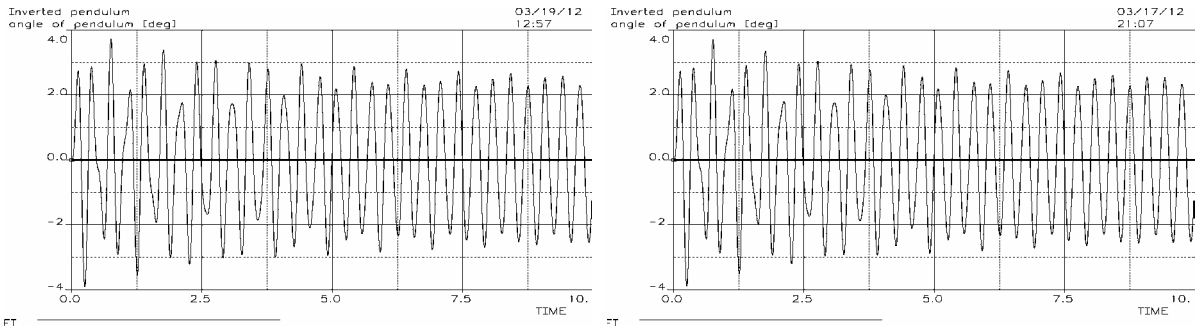

a) *b)*

Fig. 8: Time history of pendulum angle φ, excitation frequency f = 3 Hz, a) massless model, b) point-mass model.

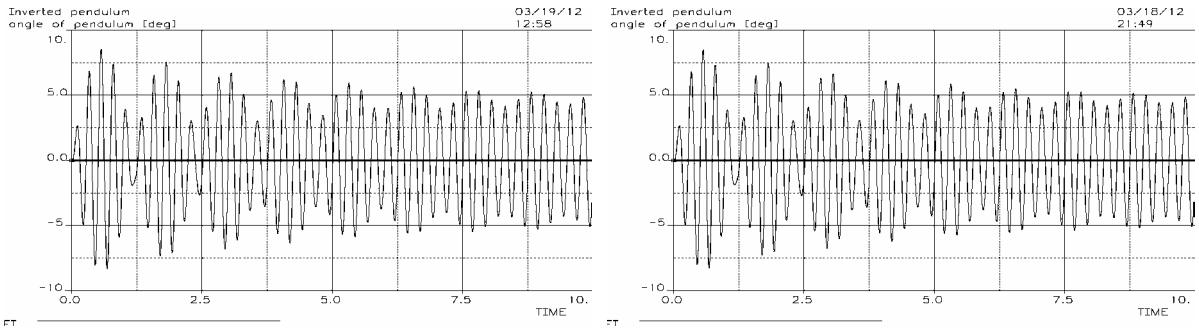

a) *b)*

Fig. 9: Time history of pendulum angle φ, excitation frequency f = 4 Hz, a) massless model, b) point-mass model.

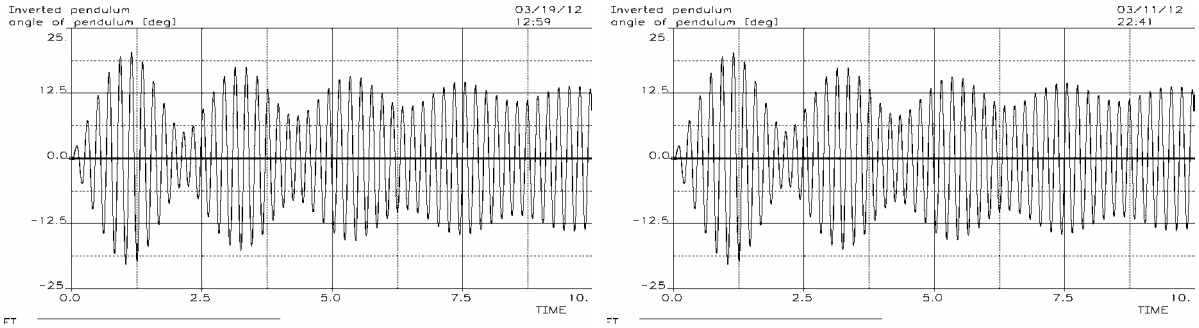

a) *b)*

Fig. 10: Time history of pendulum angle φ, excitation frequency f = 5 Hz, a) massless model, b) point-mass model.

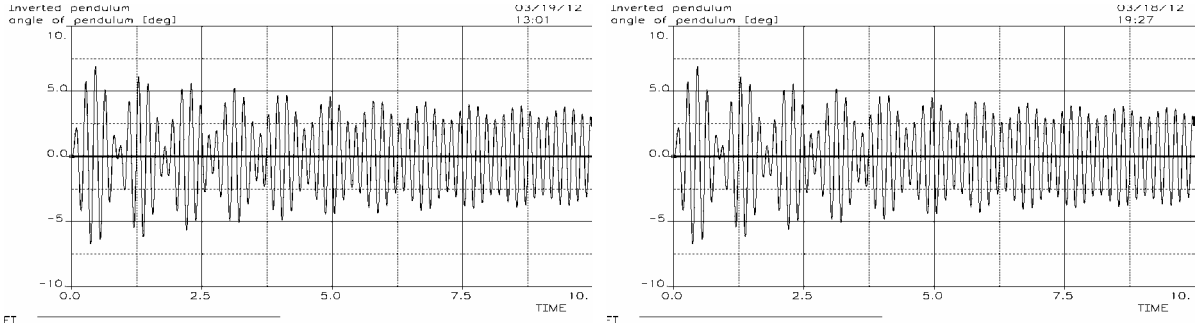

a) *b)*

Fig. 11: Time history of pendulum angle φ, excitation frequency f = 6 Hz, a) massless model, b) point-mass model.

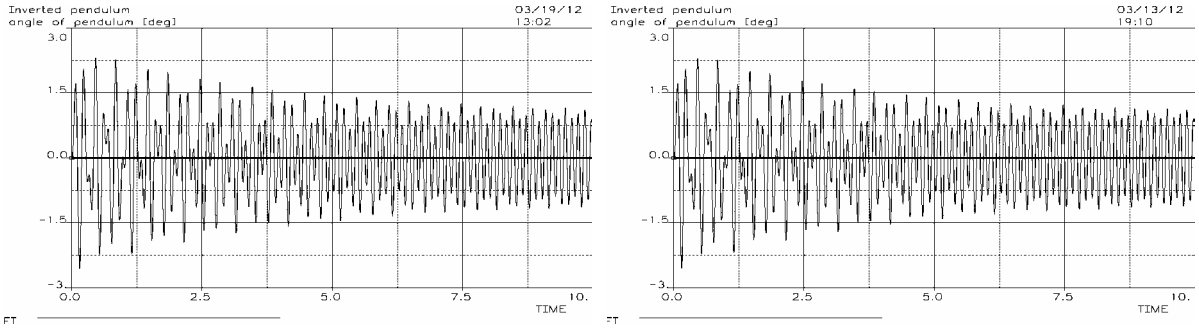

a) *b)*

Fig. 12: Time history of pendulum angle φ, excitation frequency f = 8 Hz, a) massless model, b) point-mass model.

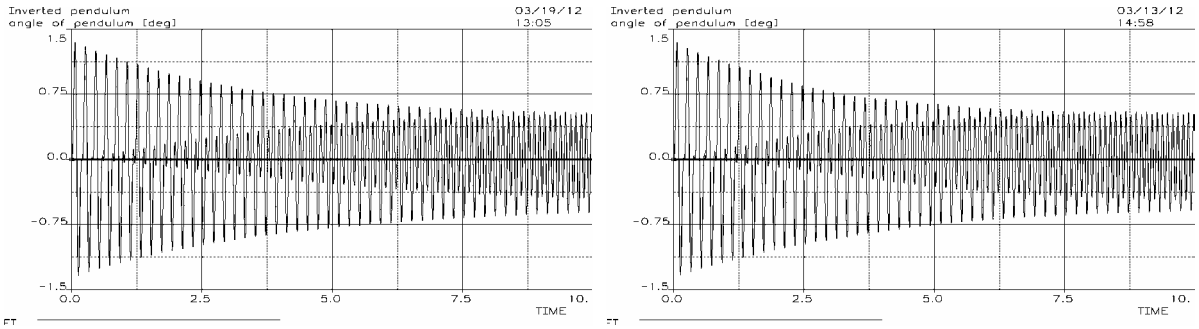

a) *b)*

Fig. 13: Time history of pendulum angle φ, excitation frequency f = 10 Hz, a) massless model, b) point-mass model.

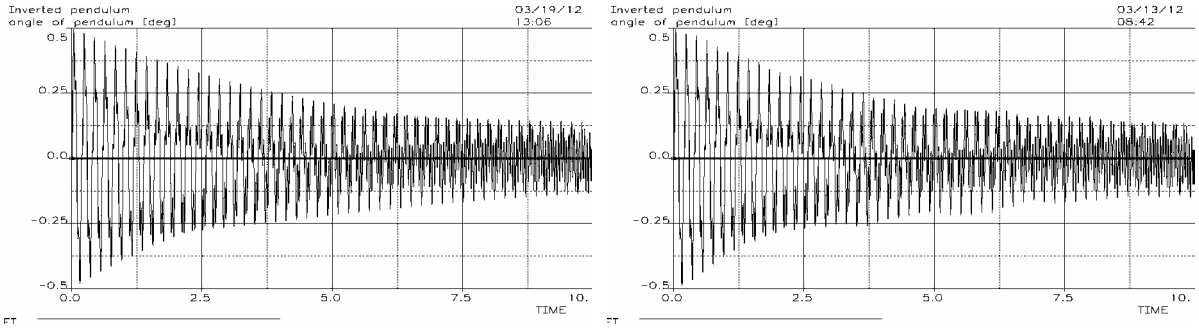

a) *b)*

Fig. 14: Time history of pendulum angle φ, excitation frequency f = 20 Hz, a) massless model, b) point-mass model.

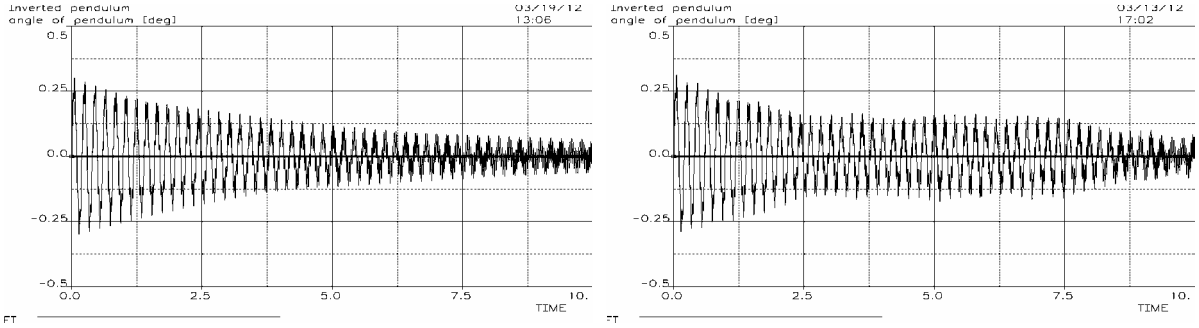

a) *b)*

Fig. 15: Time history of pendulum angle φ, excitation frequency f = 30 Hz, a) massless model, b) point-mass model.

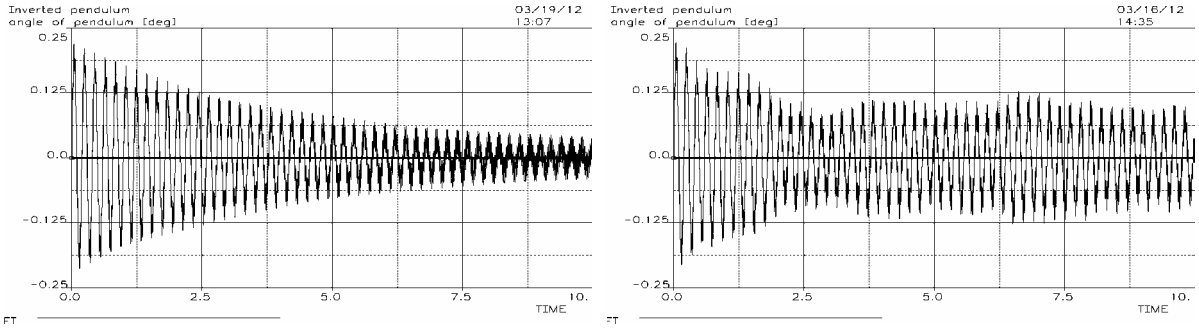

a) *b)*

Fig. 16: Time history of pendulum angle φ, excitation frequency f = 40 Hz, a) massless model, b) point-mass model.

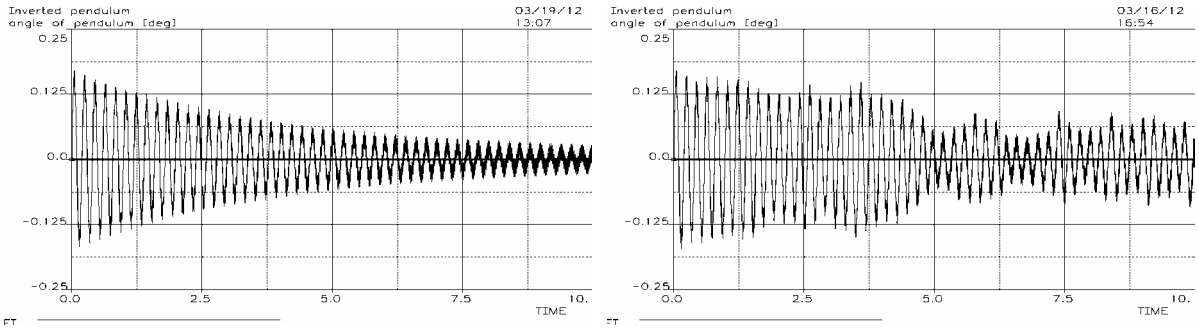

a) *b)*

Fig. 17: Time history of pendulum angle φ, excitation frequency f = 50 Hz, a) massless model, b) point-mass model.

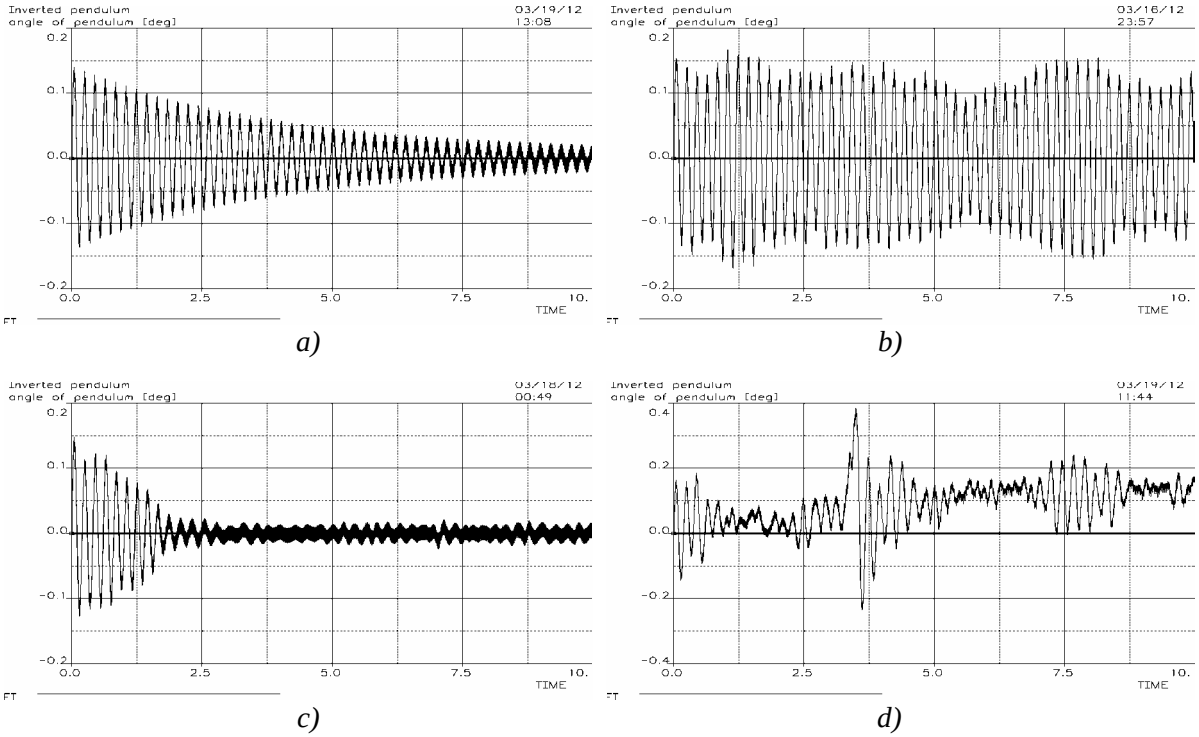

Fig. 18: Time history of pendulum angle φ, excitation frequency f = 60 Hz, a) massless model, b) point-mass model, c) point-mass model (fibre mass 0.11 grams), d) point-mass model of carbon fibre (other scale in vertical axis).

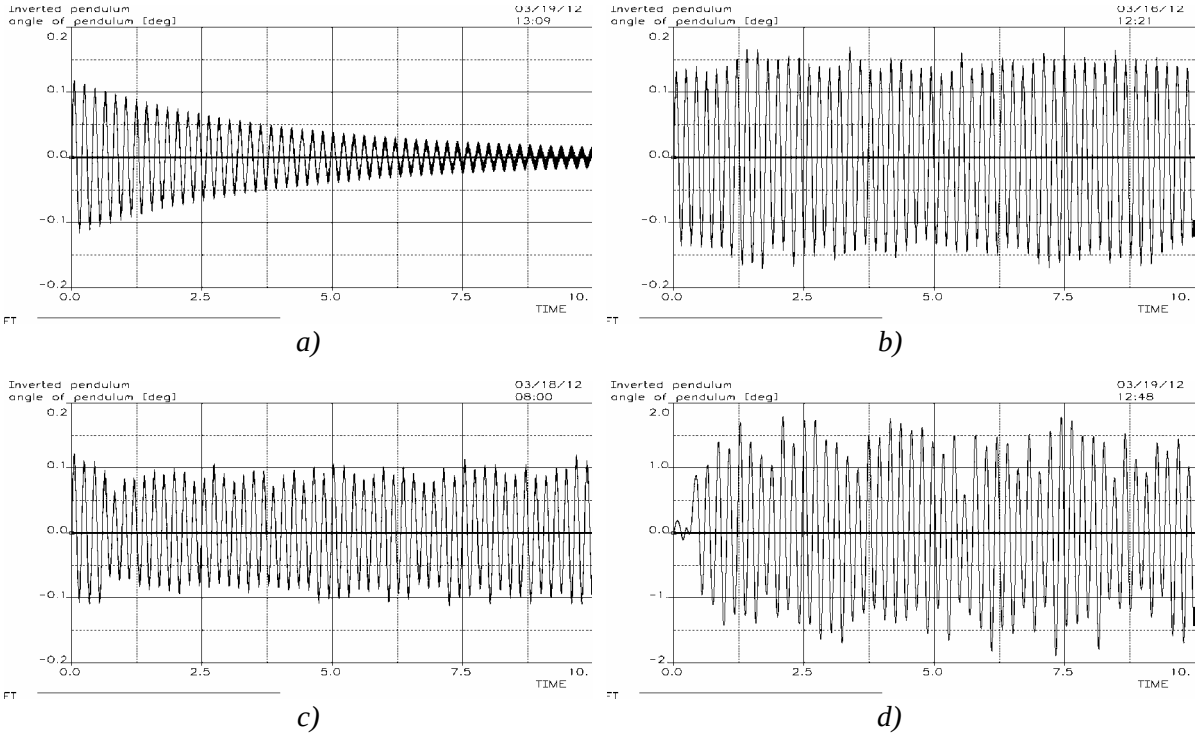

Fig. 19: Time history of pendulum angle φ, excitation frequency f = 70 Hz, a) massless model, b) point-mass model, c) point-mass model (fibre mass 0.11 grams), d) point-mass model of carbon fibre (other scale in vertical axis).

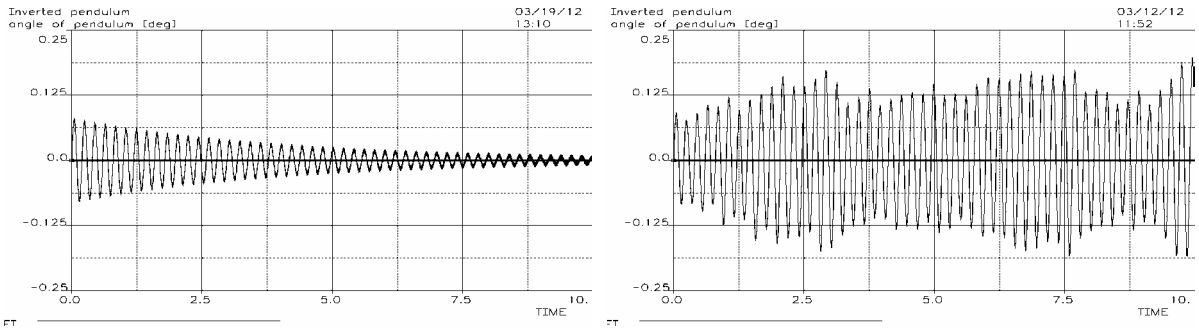

a) *b)*

Fig. 20: Time history of pendulum angle φ, excitation frequency f = 100 Hz, a) massless model, b) point-mass model.

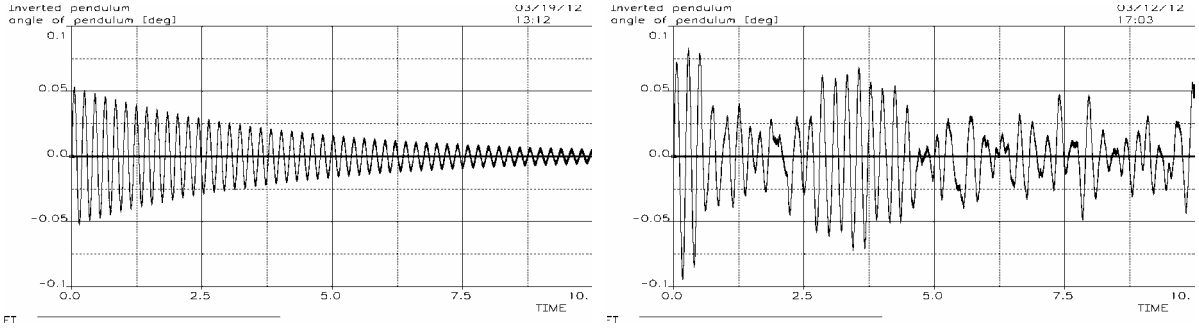

a) *b)*

Fig. 21: Time history of pendulum angle φ, excitation frequency f = 150 Hz, a) massless model, b) point-mass model.

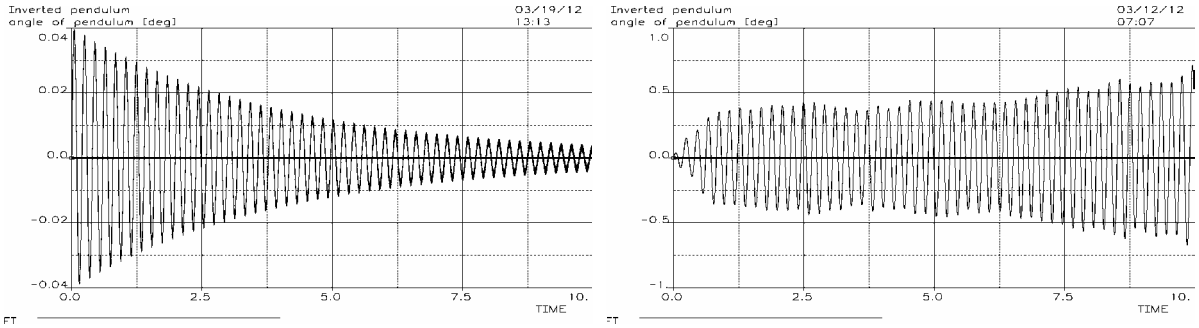

a) *b)*

Fig. 22: Time history of pendulum angle φ, excitation frequency f = 200 Hz, a) massless model, b) point-mass model (other scale in vertical axis).

6. Conclusions

The approach to the cable modelling based on the lumped point-mass representations for the investigation of the motion of the inverted pendulum was validated on the basis of the results obtained using the massless fibre model. It was proved that point-mass fibre model is well applicable up to the excitation frequency of approx. 50 Hz (which is generally sufficient for the control of the considered cable-based manipulators). At higher excitation frequencies partly vibration of individual point masses and partly probably also influence of numerical errors at solving equations of motion show up in the results of simulations. They are caused by considering almost massless fibres in the point-mass fibre model.

Experimental verification of the cable dynamics within the manipulator systems and research aimed at measuring the material properties of selected fibres are considered important steps in further research.

Acknowledgement

The paper has originated in the framework of solving No. P101/11/1627 project of the Czech Science Foundation entitled "Tilting Mechanisms Based on Fiber Parallel Kinematical Structure with Antibacklash Control" and institutional support for the long-time conception development of the research institution provided by Ministry of Industry and Trade of the Czech Republic.

References

Chan, E.H.M. (2005) *Design and Implementation of a High-Speed Cable-Based Parallel Manipulato*r. PhD Thesis, University of Waterloo.

Diao, X. & Ma, O. (2009) Vibration analysis of cable-driven parallel manipulators. *Multibody System Dynamics*, 21, 4, pp. 347-360.

Drábek, P. & Milota, J. (2007) *Methods of Nonlinear Analysis*. Birkhauser, Basel.

Freire, A. & Negrão, J. (2006) Nonlinear Dynamics of Highly Flexible Partially Collapsed Structures, in: *Proc. III European Conference on Computational Mechanics, Solids, Structures and Coupled Problems in Engineering* (C.A. Mota Soares, J.A.C. Martins, H.C. Rodrigues, J.A.C. Ambrósio, C.A.B. Pina, C.M. Mota Soares, E.B.R. Pereira & J. Folgado eds), Laboratório Nacional de Engenharia Civil, Lisbon, CD-ROM.

Hajžman, M. & Polach, P. (2011) Modelling of Cables for Application in Cable-Based Manipulators Design, in: *Proc. ECCOMAS Thematic Conference Multibody Dynamics 2011* (J.-C. Samin & P. Fisette eds), Université catholique de Louvain, Brussels, CD-ROM.

Kamman, J.W. & Huston, R.L. (2001) Multibody Dynamics Modeling of Variable Length Cable Systems. *Multibody System Dynamics*, 5, 3, pp. 211-221.

Polach, P. & Hajžman, M. (2011a) Approaches to the Modelling of Inverted Pendulum Attached Using of Fibres, in: *Proc. 4th International Conference on Modelling of Mechanical and Mechatronic Systems 2011* (A. Gmiterko ed.), Technical University of Košice, Herľany, CD-ROM (pp. 408-416).

Polach, P. & Hajžman, M. (2011b) Absolute nodal coordinate formulation in dynamics of machines with cables, in: *Proc. 27th Conference with International Participation Computational Mechanics 2011* (V. Adámek & M. Zajíček eds), University of West Bohemia in Plzeň, Plzeň, CD-ROM.

Polach, P. & Hajžman, M. (2011c) Investigation of Dynamic Behaviour of Inverted Pendulum Attached Using of Fibres, in: *Proc. 11th Conference on Dynamical Systems – Theory and Applications, Nonlinear Dynamics and Control* (J. Awrejcewicz, M. Kaźmierczak, P. Olejnik & J. Mrozowski eds), Department of Automatics and Biomechanics, Technical University of Łódź, Łódź, pp. 403-408.

Polach, P. & Hajžman, M. (2012a) Investigation of dynamic behaviour of inverted pendulum attached using fibres at non-symmetric harmonic excitation, in: *Proc. EUROMECH Colloquium 524 Multibody system modelling, control and simulation for engineering design* (J.B. Jonker, W. Schiehlen, J.P. Meijaard & R.G.K.M. Aarts eds), University of Twente, Enschede, pp. 42-43.

Polach, P. & Hajžman, M. (2012b) Effect of Fibre Preload on the Dynamics of an Inverted Pendulum Driven by Fibres, in. *Proc The 2nd Joint International Conference on Multibody System Dynamics* (P. Eberhard ed.), University of Stuttgart, Stuttgart, CD-ROM.

Polach, P., Hajžman, M., Šika, Z., Mrštík, J. & Svatoš, P. (2012) Effects of fibre mass on the dynamics of an inverted pendulum driven by cables, in: *Proc. National Colloquium with International Participation Dynamics of Machines 2012* (L. Pešek ed.), Institute of Thermomechanics Academy of Sciences of the Czech Republic, Prague, pp. 127-134.

Rachůnková, I., Staněk, S. & Tvrdý, M. (2009) *Solvability of Nonlinear Singular Problems for Ordinary Differential Equations*. Hindawi Publishing Corporation, New York.

Schmitt, K. & Thompson, R.C. (2004) *Nonlinear Analysis and Differential Equations – An Introduction*. Lecture Notes, University of Utah, Salt Lake City.

Shabana, A.A. (1997) Flexible Multibody Dynamics: Review of Past and Recent Developments. *Multibody System Dynamics*, 1, 2, pp. 189-222.

Smrž, M. & Valášek, M. (2009) New Cable Manipulators. In: *Proc. National Conference with International Participation Engineering Mechanics 2009* (J. Náprstek & C. Fischer eds)), Institute of Theoretical and Applied Mechanics Academy of Sciences of the Czech Republic, Svratka, CD-ROM (pp. 1209-1216).

Valášek, M. & Karásek, M. (2009) HexaSphere with Cable Actuation. *Recent Advances in Mechatronics: 2008-2009*, Springer-Verlag, Berlin, pp. 239-244.

Wittbrodt, E., Adamiec-Wójcik, I. & Wojciech, S. (2006) *Dynamics of Flexible Multibody Systems. Rigid Finite Element Method*. Springer, Berlin.